Pol. J. Environ. Stud. Vol. 31, No. 6 (2022), 5427-5442
DOI: *10.15244/pjoes/151110* ONLINE PUBLICATION DATE: 2022-10-20

Original Research

Optimized Pan Evaporation by Potential Evapotranspiration for Water Inflow Estimation in Ungauged Inland Plain Lake, China

Zhilei Yu[1], Huiliang Wang[1], Baisha Weng[2]*, Shuyu Zhang[3], Tianling Qin[2], Denghua Yan[2]

[1]School of Water Conservancy Engineering, Zhengzhou University, Zhengzhou, Henan 450001, P.R. China
[2]State Key Laboratory of Simulation and Regulation of the River Basin Water Cycle in River Basin, China Institute of Water Resources and Hydropower Research, Beijing 100038, P.R. China
[3]School of Environment, Southern University Science and Technology, Shenzhen, Guangdong 518000, P.R. China

Received: 4 March 2022
Accepted: 18 June 2022

Abstract

Under the climate changes and human activities, large areas of lakes shrunk and wetlands degenerated. Evapotranspiration (ET) is the primary water loss in the water balance of closed-basin and lakes. However, ET is difficult to estimate, especially in the data-scarce or ungauged zones. For a closed lake without outflow, the inflow could be used to estimate the water shortage of ecological water demand. Based on meteorology data and the pan evaporation (ET_{pan}) data, Penman-Monteith and Hargreaves Model were used to estimate potential evapotranspiration (ET_0), which was used to estimate ET, and used the water balance model to assess the water inflow of Wolong Lake. PM model proposed the satisfactory estimation of ET_0 from Wolong Lake. The empirical formula of the net radiation was built based on the coefficient that derived from data fitting with function of the measured ET_{pan} and the estimated ET_0. The temperature was the dominant factor for the increment of the ET_{pan}. In the data-scarce or ungauged zones, ET_0 could be used to evaluate the evapotranspiration from the lake surface (ET_{lake}), instead of the ET_{pan}. The results found that the inflow of Wolong Lake could not meet the demand of the evaporation and water volume advancement.

Keywords: potential evapotranspiration, pan evaporation, water balance, water inflow, inland plain lake

Highlights

Temperature was the dominant factor affecting the water loss over WL lake.

WL lake water inflow could not meet the demand of the water loss over WL lake.

ET0 could be used to evaluate the lake loss in the data-scarce or ungauged zones.

*e-mail: wengbs0906@126.com

Graphical Abstract

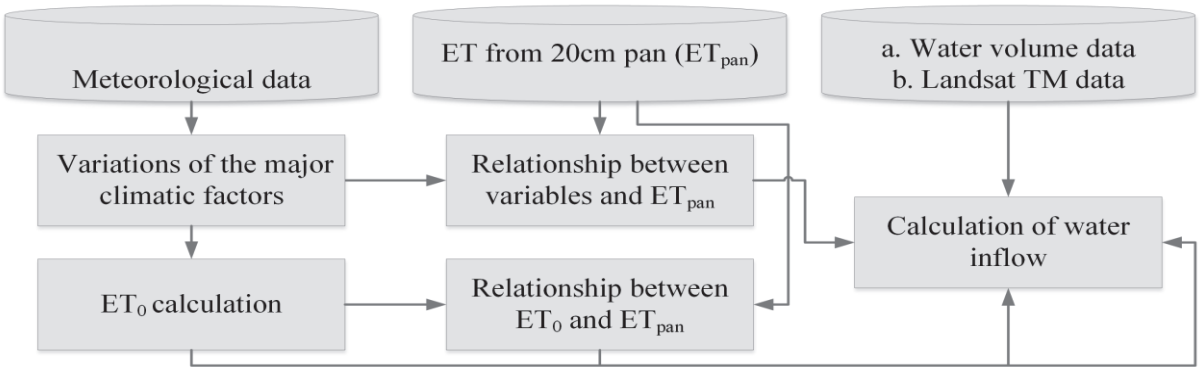

Introduction

Lake water is the key element of terrestrial water storage. Quantification of terrestrial water storage is important and useful for water resources planning and management, socio-economic development and ecological sustainability [1, 2]. It was found that extensive lakes shrink and wetlands degenerate [3-5] were partially resulted from the climate change and intensive human activities [6]. Evapotranspiration (ET) is the main water loss in the water budget of closed-basin with lakes [7-9]. The atmospheric and lake-surface processes influence the evapotranspiration from lake surface (ET_{lake}). Changes of hydro-climatic and climatic variables, such as air temperature, humidity, wind speed, and energy flux, affect the variation of ET_{lake}. Compared with climate warming from 1850 to1900, the average global surface temperature has increased by around 0.87°C from 2006 to 2015 [10]. It was assumed that temperature rising enhanced of evapotranspiration capacity and amount [11-13]. ET is a fundamental component of the hydrological and energy cycle [14, 15] that transferred 65% of precipitation back to the atmosphere [16]. For planning and management of water resource and irrigation projects, ET affects the regional water balance and decides the water demand of crops. However, ET is difficult to measure and parameterize [16-18]. The current observations were not enough to the research on ET. The requirement to estimate the crop water demand, support the irrigation management and hydrological predictions cannot be satisfied, especially in ungauged regions.

The estimation of ET usually refers to the potential evapotranspiration (ET_0) [13, 19], which was defined as the amount or rate of water evaporated from a large area without any water supply limitation or any vegetation stress [20, 21]. ET_0 is a climatic element that can effectively depict the capacity and energy of evapotranspiration, assuming no limitation on water supply [22]. Meanwhile, it is also a characteristic variable in hydro-climatic water cycle, an important parameter in irrigation system planning and scheduling, and a robust input of hydrological models [23], as well as an essential part of water balance [24]. Thus, it is vital to estimate the ET_0.

Massive physical, empirical and semi-empirical models can estimate the ET_0 in a specific region. Recommended by Food and Agriculture Organization (FAO), Penman-Monteith formulation has been implemented widely in hydrological, agricultural and hydro-climatic fields [25-27]. Thornthwaite equation was also proposed and has been widely used to estimated ET [24, 28]. Hargreaves model could estimate ET_0 with limited climatological dataset [29, 30]. Among the various methods, different studies have developed the specific measurement to simulate ET_0, such as combination models [31], temperature-based models [28] and energy-based models [29].

In recent years, numerous studies focus on documenting the spatial-temporal variations of ET_0 [32-34], comparison of ET_0 estimation methodology [16, 21], the environmental and climatic driving factors of ET_0 [35-37], influences of land use on ET_0 [23, 38, 39] and other hydrological and agricultural fields [36, 40]. For example, Han et al. [41] proved that 1991 was a shift point of ET_0 in the Jing-Jin-Ji region that annual ET_0 decreased before 1991 and increased after 1991. Xu and Singh [19] employed eight radiations-based models to estimate ET_0 and selected the model that agreed most with pan evaporation (ET_{pan}) that measured over a pan with diameter of 20 cm in the north-western Ontario.

Most studies used the dynamic water balance model to investigate the variation of the water volume (or level) at the annual, seasonal, and monthly scales [42-44]. Gibson et al. [45] examined the potential impacts of the water levels variation of Great Slave Lake from 1964 to 1998. Wale et al. [46] estimated the contributions of runoff from ungauged catchment to Lake Tana's water balance. Xu et al. [47] explored the change of runoff and water level of Poyang Lake. These researches needed to obtain the data of discharge (involving both surface and groundwater runoff), precipitation and evaporation. However, for the lake (or reservoir) water balance, few studies have documented the arithmetic of water inflow by using ET_0, especially in the data-scarce or ungauged zones. Therefore, how to evaluate the water loss through ET_0 from a lake in the ungauged zones? Whether ET_{pan}

could be optimized through the estimation of ET_0? And what is the relationship between ET_0 and ET_{pan}? All the above questions are needed to be answered and will solve in the study.

To answer the above questions, this study estimated the ET_0 through two widely-used models (Penman-Monteith (PM) Model and Hargreaves (Har) Model), as well as the inflow of inland plain lake water through a water balance model. The objectives of this study are as follows: (a) to explore the dynamic traits of climatic factors in the study region; (b) to investigate the relationship between ET_{pan} and climatic factors; (c) to recalibrate the accuracy of ET_0 through local ET_{pan} observation data and deriving the coefficient to optimize empirical formula of net radiation (R_n); and (d) to estimate the inflow of the lake based on ET_0. The results and conclusions of this study is helpful to fill in gaps in the measured hydrological data.

Material and Methods

Study Site

Wolong Lake (WL), as a wetland, is the ecological barrier and site for birds migrating [48]. Studies asserted that wetlands stored 15% of total carbon over the Earth and played a significant role in ecological balance [49, 50]. Affected by climate changes and human activities, extreme hydrological events occurred more frequently and intensively [51, 52]. With insufficient water resources and intensive water consumption, the inflow of WL is seriously squeezed in the region. Water level of the WL affected the birds and their habitat [48].

As shown in Fig. 1, WL (42°39′-42°46′N, 123°7′-123°19′E), located in Kangping county, which has an area of 50.54 km^2 and is the largest freshwater lake in Liaoning province and the second largest in Northeast China. WL reservoir volume has changed from 6, 289.7 × 10^4 m^3, 5,308.6 × 10^4 m^3 and 4, 615.0 × 10^4 m^3 in 2015, 2016 and 2017. Large areas of WL had shrunk. As a semi-artificial and semi-natural wetland, WL (also known as Xipaozi Reservoir) was built in 1958 that stores water from East and West Malian River and flows into the Liao River. Liao River is the largest river in Liaoning Province. WL is vital ecological green core for eastern Asia birds' migration and for migratory birds' propagation [53]. In 2001, it was listed as a provincial natural protection area. WL Natural Scenic Resort was established to protect the waterfowl habitat and water biological resources. As recorded, More than 75% White Cranes rest here in the migration season of 2008 to 2009.

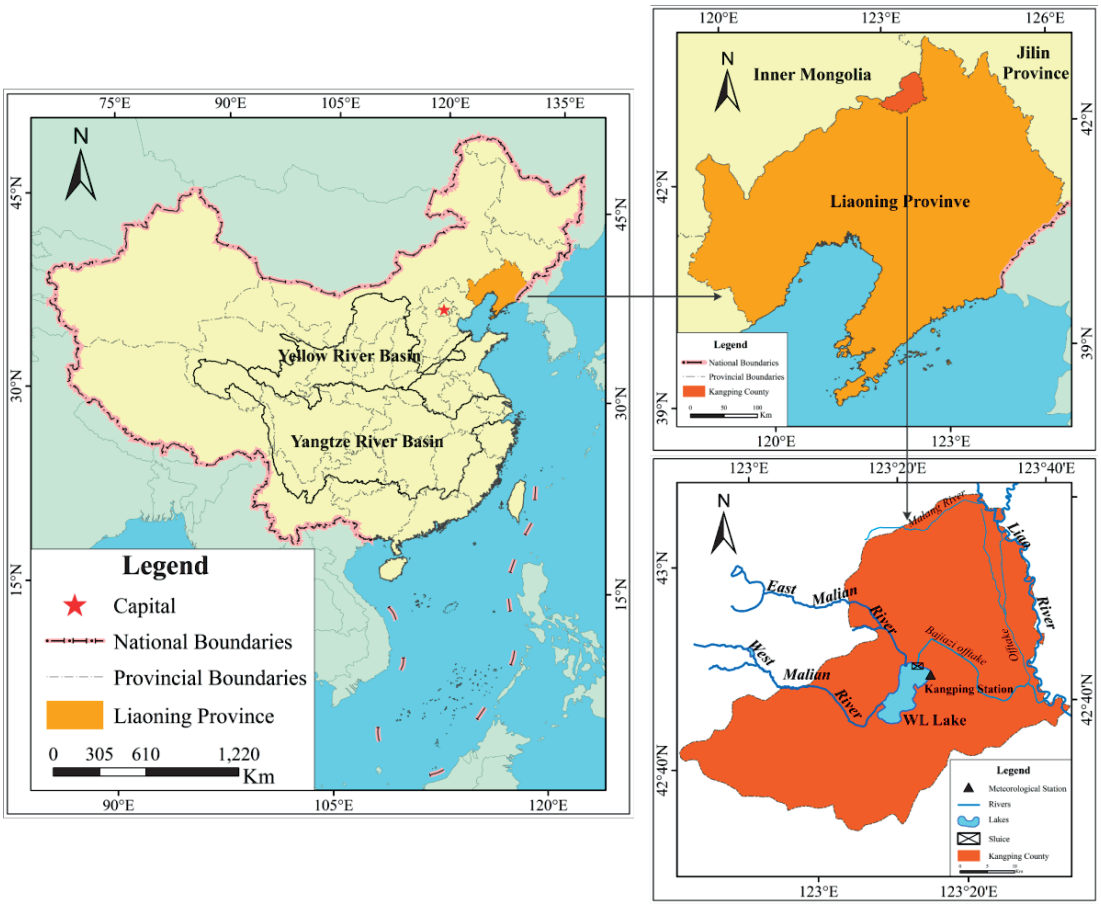

Fig. 1. Location of the WL Lake.

Table 1. Basic parameter information of the Kangping national meteorological station.

Parameter name		Mean Annual Value	Data Duration
Precipitation	Pe	522.52 mm	1960.1.1 – 2016.12.31
Average air temperature	T_{mean}	7.5ºC	1960.1.1 – 2016.12.31
Minimum air temperature	T_{max}	13.1ºC	1960.1.1 – 2016.12.31
Maximum air temperature	T_{min}	2.5ºC	1960.1.1 – 2016.12.31
Sunshine duration	SD	227.8 h	2000.1.1 – 2016.12.31
Wind speed	WS	3.0 m/s	2000.1.1 – 2016.12.31
Relative humidity	RH	60%	2000.1.1 – 2016.12.31
20 cm pan evaporation	ET_{pan}	1973.9 mm	1960.1.1 – 2013.12.31

WL is an important environmental protection zone in the area. It is not only an ideal transit depot in migration for birds but also an ecological shield for the Northwest Liaoning Province. However, with insufficient water resources and high water consumption, the inflow of WL is seriously squeezed. Meanwhile, the intensity and frequency of drought events increases under climatic change. The ecological water demand of WL is not satisfied for a long time. The ecological environment of WL has deteriorated and its ecological security protection foundation has been fall behind. The retrograde ecological succession has taken place and the ecosystem service function has seriously deteriorated, which threatened the ecological security in northwest Liaoning Province.

Measurements and Data Processing

Daily observation from the Kangping national meteorological station (42°45′N, 123°20′E) (Fig. 1) were collected as the basic data and training set, including the daily precipitation (P_e) from 1961 to 2016, daily average air temperature (T_{mean}), daily minimum (T_{min}) and maximum (T_{max}) air temperature from 1961 to 2016, sunshine duration (SD) from 2000 to 2016, wind speed at 10 m height (WS) from 2000 to 2016, relative humidity (RH) from 2000 to 2016, and 20 cm pan evaporation (ET_{pan}) from 1960 to 2013 (Table 1). Basic parameter information of the meteorological data was shown in Table 1. Considering the spatial-scales of the study area, the Kangping national meteorological station data was used to represent the hydro-climatological characteristics of the whole study area.

The variation of area of WL from 1995 to 2017 was extracted from the Landsat TM data (30 m × 30 m), National Aeronautics and Space Administration (NASA) (https://search.earthdata.nasa.gov). The monthly water volume of WL in 2015 and 2016 were also collected as an input of water balance model.

The flowchart of this study is shown in Fig. 2. The temporal variations of major climatic factors and ET_{pan} in WL were investigated at first. Secondly, the Penman-Monteith (PM) Model and Hargreaves (Har) Model were explored to estimate the ET_0. Then the relationship between ET_0 and ET_{pan} was established and evaluated. Based on the water balance model, ET_0 was used to estimate the inflow of WL (Fig. 2).

Models

Penman-Monteith (PM) Model

The FAO PM equation has been widely applied to derive ET_0 [25, 54, 55], whose performance has been widely validated [56]. The PM equation is shown as Eq. (1).

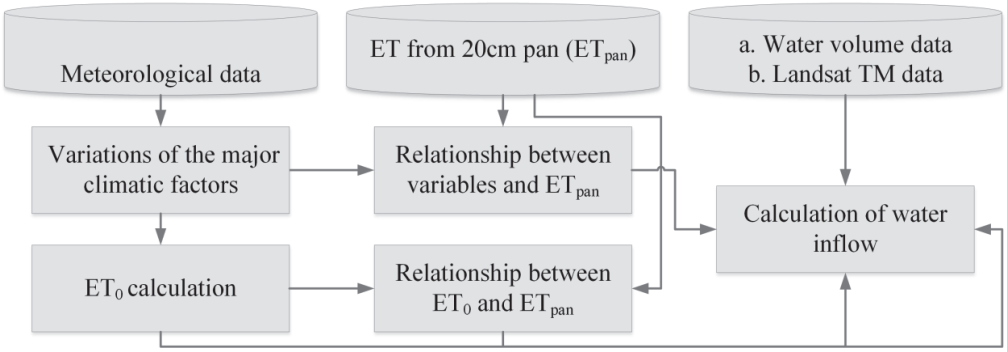

Fig. 2. Flowchart of the investigation of water inflow calculation.

$$ET_0 = \frac{0.408\Delta(R_n - G) + \gamma \frac{900}{T+273} u_2 (e_s - e_a)}{\Delta + \gamma(1 + 0.34u_2)} \quad (1)$$

where ET_0 is the daily potential evapotranspiration rate (mm d^{-1}); G is the soil heat flux density (MJ m^{-2} day^{-1}); T is the mean daily air temperature at 2 m height (ºC); U_2 is the mean 24^{-h} wind speed at 2 m height (m s^{-1}); e_s and e_a is the saturated and actual vapor pressure respectively (kPa); γ is the psychometric constant (kPa $ºC^{-1}$); Δ is the slope of vapor pressure (kPa $ºC^{-1}$) and Rn is the net radiation at the ground surface (MJ m^{-2} day^{-1}).

The R_n [57]can be expressed as:

$$R_n = R_{ns} - R_{nl} \quad (1\text{-}1)$$

$$R_{ns} = (1 - \alpha) R_s \quad (1\text{-}2)$$

$$R_s = (a_s + b_s \frac{n}{N}) R_a \quad (1\text{-}3)$$

where R_{ns} is the net short-wave radiation (MJ m^{-2} day^{-1}); R_{nl} is the net outgoing long-wave radiation (MJ m^{-2} day^{-1}); R_s is the incoming solar radiation (MJ m^{-2} day^{-1}); R_a is the extraerrestrial radiation (MJ m^{-2} day^{-1}); α is the albedo coefficient; a_s and b_s are regression constants and are set to the original empirical values 0.25 and 0.50, respectively; n represents actual daily sunshine duration (h); N is the maximum possible sunshine duration at Kangping station (h); n/N means the relative sunshine duration.

The wind speed at 10 m height was converted to the wind speed at 2 m above the ground surface to estimate ET_0 through:

$$U_2 = U_z \cdot \frac{\ln(2/z_0)}{\ln(z/z_0)} \quad (1\text{-}4)$$

where U_2 is the wind speed at a height of 2 m above the surface (m s^{-1}); U_z is the wind speed at z m height (m s^{-1}), and z_0 is the surface roughness height = 0.002 m for water.

Hargreaves (Har) Model

Har model can be described as Eq. (2) [21].

$$ET_0 = 0.0023 \frac{R_a}{\lambda} (T_{\max} - T_{\min})^{0.5} (T_{mean} + 17.8) \quad (2)$$

where T_{mean}, T_{max} and T_{min} are the daily mean, maximum, and minimum temperature (ºC), respectively; R_a is the daily extraterrestrial radiation (MJ m^{-2} day^{-1}); and λ is the latent heat of vaporization (2.45 MJ kg^{-1}).

Water Balance Model

Except for two sluices in the south and north of the lake for flood management, there is no other channel connecting WL with outside region. WL was treated as a closed-basin lake in this study. For a closed-basin, precipitation and runoff are the main water sources, and evaporation is the main water loss [58]. Reservoirs and farmlands all locate in the upper reaches of WL intercepting the inflow. In addition, no hydrological monitors were set along the river side. Thus, for a closed-basin lake, the basic hydrologic balance model must balance the precipitation for inputs and evaporation for outputs [2]. Water inflow could be estimated from the water balance model [59-61]. The water balance equation in WL can be expressed as the following:

$$P + R - ET - I = \pm \Delta W \quad (3)$$

$$WI = P + R \quad (4)$$

where P is monthly precipitation within the lake (10^4 m^3); R is monthly runoff (10^4 m^3) containing both the surface and groundwater runoff; ET is monthly evaporation from lake surface (10^4 m^3), as the main water loss in WL; ΔW is monthly mean variation of lake volume (10^4 m^3); WI is the water inflow of WL (10^4 m^3). Based on the records from technical literatures and geophysical reports, the geological structure of WL bottom is the tertiary period sandstone, with infinitesimal permeable ability. It was treated as impervious bed and the infiltration loss of lake is zero: I = 0. The water balance model is usually used as a basic technique to estimate ET for a catchment area [62]. In turn, combined the water volume variation, ET is used to calculate the water inflow in WL.

Evaluation of Model Performance

Among empirical methods to estimate the ET_0, different equations may have different definitions. Different definitions of models need to extract different initial conditions and cause the different results. To evaluate the performance of different models in estimating ET_0, several criteria were used to include the Nash-Sutcliffe efficiency coefficient (NSE), the root mean square error (RMSE), the mean absolute error (MAE), and the coefficient of determination (R^2) [23, 63, 64]. These criteria are calculated as follows:

$$NSE = 1 - \frac{\sum_i^N (obs_i - sim_i)^2}{\sum_i^N (obs_i - \overline{obs})^2} \quad (5)$$

$$RMSE = \left(\frac{1}{N} \sum_i^N (obs_i - sim_i)^2 \right)^{0.5} \quad (6)$$

$$MAE = \frac{1}{N}\sum_{i}^{N}\left|obs_i - sim_i\right| \quad (7)$$

$$R^2 = \frac{\left[\sum_{i}^{N}(obs_i - \overline{obs})(sim_i - \overline{sim})\right]^2}{\sum_{i}^{N}(obs_i - \overline{obs})^2 \sum_{i}^{N}(sim_i - \overline{sim})^2} \quad (8)$$

where obs_i is the observed ET_{pan} (mm/day) and sim_i the estimated ET_0 (mm/day), and N is the number of observations (days). According to the previous advancements, simulation results are considered to be good for NSE≥0.75; NSE between 0.75 and 0.36 the simulation results are considered to be satisfactory [65]. NSE between 0.6 and 0.8 indicate that the model performs reasonably well [46]. NSE The closer to 1 NSE is, the better performance of the model has [64]. When R^2>0.6 and |RE|<15%, the model can be applied in the study area [66].

Results and Discussion

Changes of Climatic Factors

Fig. 3 and Table 2 show the temporal variability of the annual climatic factors in WL. At annual scale, P_e, T_{mean}, T_{max}, T_{min} and SD show increasing tendency, while ET_{pan}, SW, and RH decreased. This is consistent with the study about climatic variation trends in Northeast China [67]. Annual P_e increased slightly by 6.78mm per decade during the 1960-2016. Mean annual P_e was around 52 2mm and precipitation concentrates in rainy season from June to August. The highest value of annual Pe was over 840 mm in 1998 and the lowest was less than 310mm in 1982. Annual T_{mean}, T_{max} and T_{min} increased at rates of 0.31ºC, 0.15ºC and 0.42ºC per decade from 1960 to 2016, respectively. Annual T_{mean} was 7.54ºC and the variation range of annual T was 0.47ºC to 14.72ºC. ET_{pan} decreases by 44.76mm per decade from 1960 to 2013. The multi-year average of annual ET_{pan} was about 1974 mm. Annual SW was 3 m s^{-1} and annual RH was around 60%. Annual SW decreased sharply by 0.4 m/s per decade, and annual RH also shows the decreasing trend at a rate of 0.27% per decade.

Fig. 4 shows the seasonal variations of key climate factors in the WL. Variables changes showed temporal differences in seasonal distribution. Changes of the P_e, T_{mean}, ET_{pan} and SD showed the single-peak trends from the seasonal variation. Except ET_{pan}, other variables revealed as follows: summer had median maximum value and winter had minimum value. Seasonal changes of T_{mean} performed relative concentration. RH and WS changed oppositely in boxplots which had low-high and high-low peaks, respectively. Except T_{mean}, influenced mainly by RH and WS, the variation of the ET_{pan} was larger in spring than in summer. Compared with other three seasons, WL need more water inflow to meet its ecological water demand because ET_{pan} and water loss was strongly and fiercely in the spring.

Table 2. The slope and Z-Values of linear regression in various climatic factors.

Climatic factors	Slope/10a	Z-Value
P_e	6.78	0.97
T_{mean}	0.31***	9.08
T_{max}	0.15***	4.62
T_{min}	0.42***	12.02
ET_{pan}	-44.76***	-3.46
WS	-0.40***	-3.88
SD	0.02	0.84
RH	-0.27*	-1.80

* significance level of 0.1; ** significance level of 0.05; *** significance level of 0.01.

Relationship between ET_{pan} and other Climatic Factors

ET was affected by multiple climatic elements, such as T (temperature), SD, RH and SW. R^2 and partial correlation coefficient were used to illustrate the mutual relationship between ET_{pan} and meteorological variables from 2000 to 2013, shown in Fig. 5 and Table 2.

Table 3 shows that T_{mean}, WS and SD had a strong positive correlation with ET_{pan} at the 0.01 significance level, while RH was negatively correlated with ET_{pan} at the 0.05 significance level. Among the meteorological variables, T_{mean} was the most sensitive factor, followed by WS, SD and RH. P_e also affected the ET_{pan}. Previous studies concluded that the precipitation caused higher RH, but led to relative low vapor pressure [57], which means the precipitation had an inhibitory effect on ET to some extent. Gharbia et al. [16] found that the decreased precipitation in winter could reduce summer precipitation of the next year and increase ET. Thus, the concrete relation between P_e and ET in need to be studied in future researches.

Fig. 5 showed that the monthly ET_{pan} is relatively higher from April to July, accounting for 50%-60% of total annual ET_{pan}. The summer monthly P_e account for 50%-80% of total annual P_e. The monthly RH is high in summer, while the monthly SD is lower in JJA (June, July, and August). The monthly highest T, varying from 20.43ºC to 26.26ºC, mainly occurred in JJA. The monthly WS is high in April and May and low in August, September and January.

T was the dominant factor for the increases of ET_{pan}, followed by WS and SD. On the contrary, RH has negative effects on ET_{pan}. P_e, T and RH are in phase,

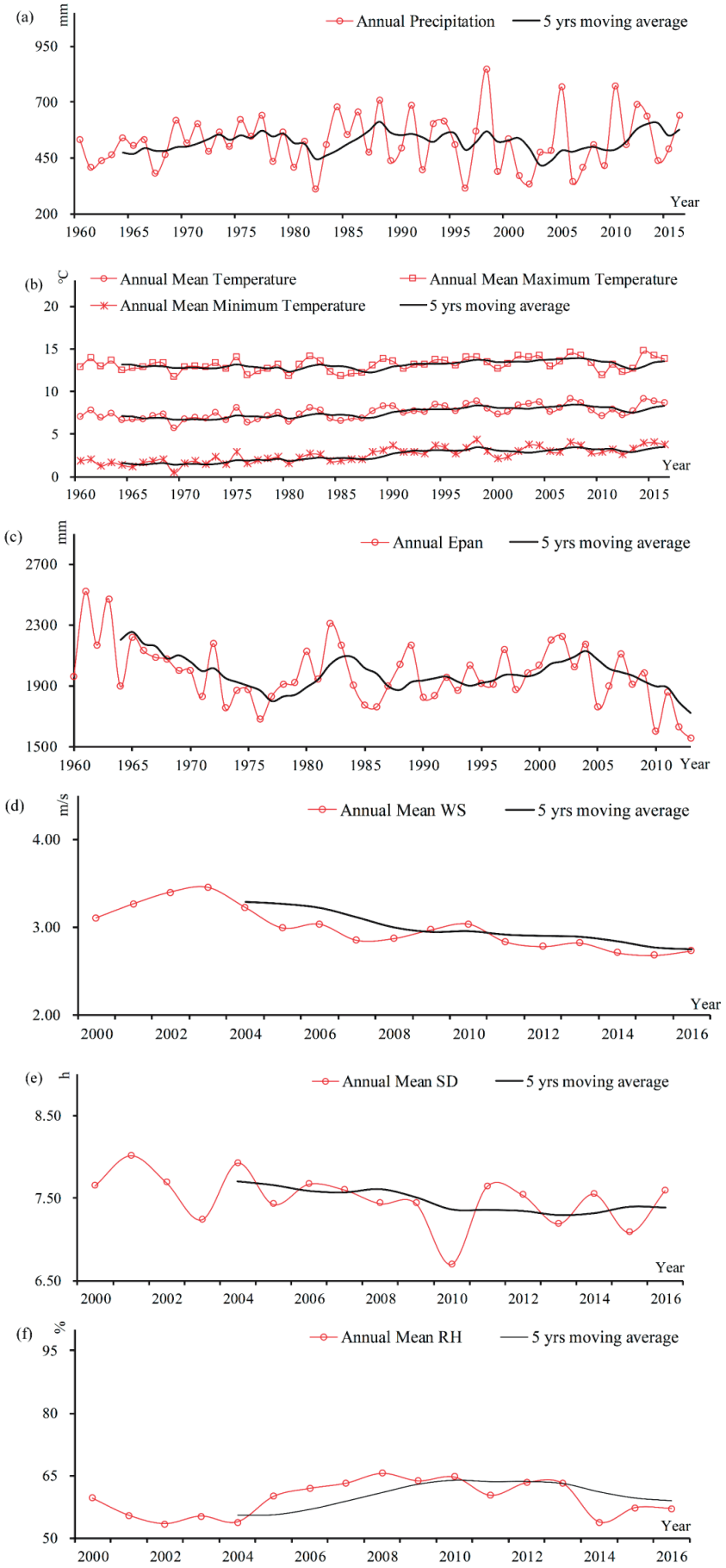

Fig. 3. Annual mean and 5-year average of a) Pre, b) T_{mean}, T_{max} and T_{min}, c) ET_{pan}, d) WS, e) SD and f) RH in WL Lake.

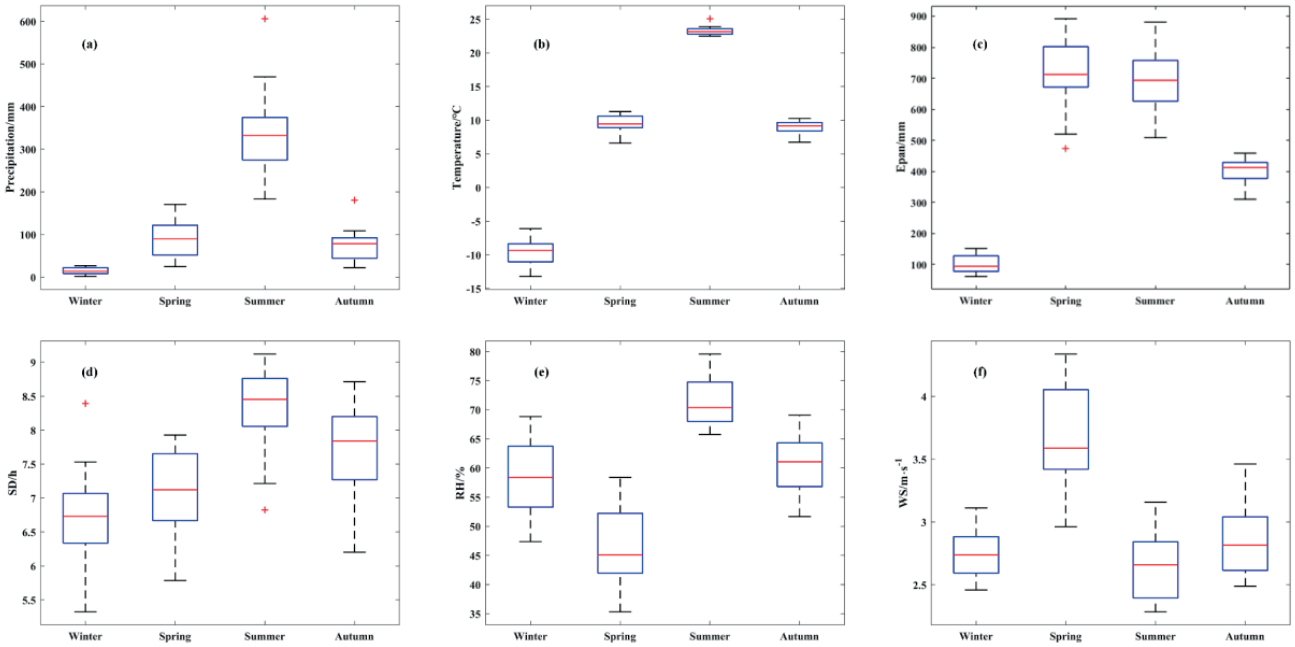

Fig. 4. Boxplots of the major climatic indexes for each season. Red lines represent the median values. Blue boxes represent ranges from the 1st quartile to the 3rd quartile. Dotted lines show the ranges of minimum and maximum. The red '+' represents outliers.

while the peak of T lagged behind ET_{pan}. However, a comprehensive relationship existed between ET0 and climatic factors. The dominant meteorological variable varies with regions. He et al. [68] showed that P_e mainly drove the inter-annual variation of land ET during 1982 to 2014 in the Loess Plateau. But SD mainly drove the daily ET of farmland in the Loess Plateau [69]. Feng et al.[70] reported that T was the most influential parameter on ET_{pan}, which was in accordance with this study. Yang &Yang [67] argued that the global SD and WS were the principal factors affecting changing ET_{pan} around China. Fan & Thomas [71] found that WS was the most influential climatic variable related to ET variability. Other studies show that T and SD were the main dominator of ET_{pan}[72, 73].

Relationship between ET_0 and ET_{pan}

Due to the lack of observed ET_{pan} after 2014, the daily ET_{pan} was calculated by daily ET_0. Two methods were applied to calculate the daily ET_0 for 13 years (2000-2013) and a linear regression model was employed to correlate ET_{pan} to further investigate the rationality of ET_0 estimation. Fig. 6 presented the regression together with the cross-correlation (R^2) between daily ET_{pan} and estimated daily ET_0 by two methods. Fig. 6 indicated that PM Model has better performance with R^2 of 0.89, while the Har Model has lower R^2 as 0.68. Table 4 showed the estimated ET_0 by two methods The results demonstrated that PM model proposed a satisfactory estimation of ET_0 in WL. For the PM model, NSE was 0.45, RMSE was 3.19% and MAE was 2.23%, which is better than that of Hargreaves model (NSE = 0.10, RMSE = 4.08%, MAE = 2.89%.).

As Har model uses only temperature in the estimation, it may fail in capturing the characteristics of evapotranspiration with extreme humidity and wind environments [19, 74]. In this study, WS is the secondary dominant factor of ET_0. Except P_e, PM model contained multiple meteorological elements, such as T, SD, RH and SW. Meanwhile, this method was considered as a standard equation and tested worldwide [64]. Thus, PM model was recommended to evaluate ET_0 in this study.

When applying the PM model, R_n is calculated at first. Several studies suggested the site-specific empirical coefficients when estimating the R_n. Makin et al. calibrated coefficients a_s and b_s as 0.26 and 0.48, respectively, through a local experiment conducted

Table 3. Correlation coefficients and Partial correlation coefficients between ET_{pan} and other meteorological factors.

	Pe	T_{mean}	WS	SD	RH
Correlation Coefficients	0.307***	0.830***	0.408***	0.640***	-0.167**
Partial Correlation Coefficients	-0.123	0.834***	0.401***	0.270***	-0.27***

* significance level of 0.1; ** significance level of 0.05; *** significance level of 0.01.

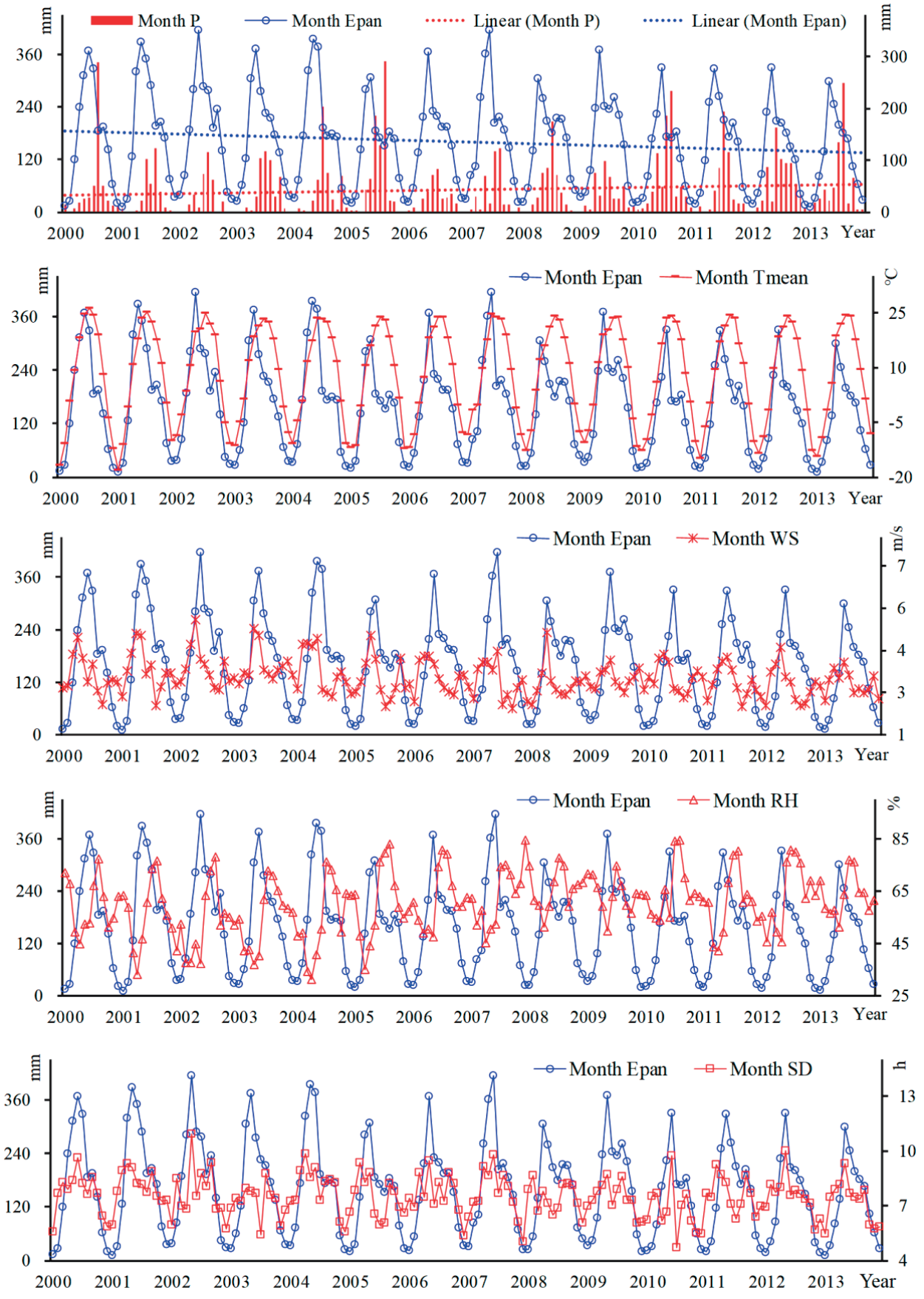

Fig. 5. Monthly variations of climatic variables and ET_{pan} in WL Lake during 2000 to 2013 (* significance level of 0.1; ** significance level of 0.05; *** significance level of 0.01.)

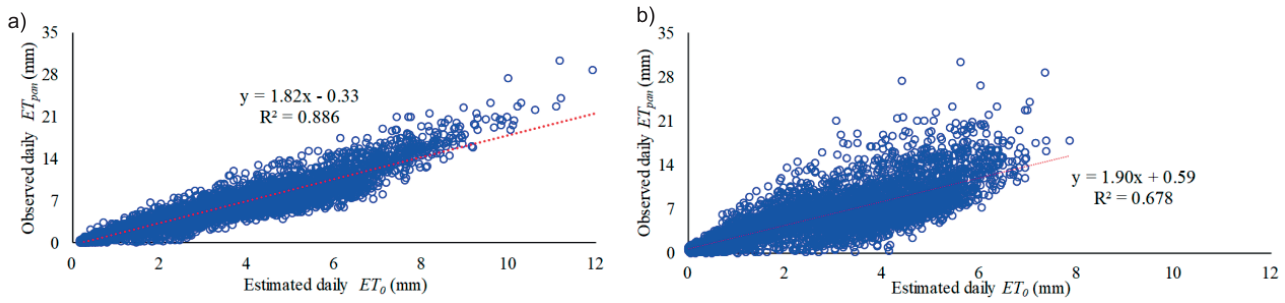

Fig. 6. Comparison of ET_{pan} and estimated ET_0 for a) PM Model (equation 1) and b) Har Model (equation 2). The original empirical values (a_s and b_s) were applied in the calculation of R_n.

between February and May, 1974, at a daily time-step [75]. FAO proposed the original constant values (a_s = 0.25; b_s = 0.50) [25]. Louche et al. estimated the values of a_s and b_s (0.206 and 0.546) at a French Mediterranean site [76]. The CGMS model simulated R_n for Spain and found a_s = 0.253 and b_s = 0.502 [77]. Podesta et al. recommended the a_s and b_s varied values in various month when calculating the R_n [78]. China territory is expansive and crosses multiple climatic zones. Therefore, the R_n formulae is modified by comparing the ET_{pan} and ET_0. PM model was applied to estimate the daily ET_0 for 8 years (2000-2008) and a linear regression equation was used to correlate with ET_{pan}. Then the coefficient linear regression equation k was determined at around 1.86. According to previous discussion, six sets of parameter values were proposed to evaluate ET_0 for 8 years (2000-2008). k was used to optimized the formula of R_n to calculate ET_0 for 4 years (2009-2013). Finally, results from models were compared using the NSE, RMSE, MAE and R^2.

A comparison of the original model parameter constants with the recalibrated values was shown in Table 5. Small errors were expected when applying the modified constants in empirical formula. Although R^2 shows slightly decreased, the original equations were also modified to improve results with the recalibrating constants as a whole. When applying the original constant values, of the three sets ((i), (iii) and (v)) evaluation resulted in validation (2000-2008) and modification (2009-2013) metrics showed a significant bias. NSE values were less than 0.5 in validation and 0.6 in modification. RMSE values were over 3% in validation and less than 3% in modification. MAE values were higher than 2% in validation and less than 2% in modification. When optimizing the R_n equation with coefficient k of the three sets ((ii), (iv) and (vi)) evaluation resulted in validation (2000-2008) and modification (2009-2013) metrics showed a significant improvement. NSE values were more than 0.75 in two periods. RMSE values were less than 2.5% in validation and less than 2% in modification. MAE values were less than 1% during two periods.

Table 4. Comparison of Nash-Sutcliffe efficiency coefficient (NSE), the root mean square error (RMSE), the mean absolute error (MAE) and the coefficient of determination (R^2) for relationship between daily estimated ET_0 and observed ET_{pan} using two methods for estimated ET_0.

	NSE	RMSE (%)	MAE (%)	R^2
Penman-Monteith Model	0.45	3.19	2.23	0.89
Hargreaves Model	0.10	4.08	2.89	0.68

Although the arithmetic errors still existed, the R_n formula was properly calibrated that could give the satisfactory ET_0 estimation (Eq. 5). With properly determined constant values, the set (vi) was selected for ET_0 evaluation.

$$R_n = k \cdot (R_{ns} - R_{nl}) \tag{9}$$

Calculation of Water Inflow

Estimation of Precipitation

From the observations from the Kangping meteorological station close to WL, precipitation on the lake surface was 435.4 mm, 491.1 mm and 637.9 mm in 2014, 2015, and 2016, respectively. The precipitation increased, which was consistent with findings in Section 3.1.

Estimation of WL ET_{lake}

ET is a major component and loss of the lake water balance. Its the variation of ET was estimated and measured indirectly. The World Meteorological Organization (WMO) suggested that a Russian GGI-3000, a 20 m^2 evaporation tank, and a Class A evaporator from the USA could measure free water surface evaporation [79]. E601 and D20 evaporation pan were constructive, efficient, and widely used in China [13, 80]. The E601 evaporator, as for a modified GGI-3000 evaporator, was a standard evaporator in China [79]. Therefore, ET_{pan} was converted into evaporation of E601 evaporator by conversion coefficients to evaluate the water surface evaporation of WL.

Table 5. Comparison of predictions NSE, RMSE, MAE and R2 values for estimating ET0 considering various constants.

	Parameter	Validation (2000-2008)				Modification (2009-2013)			
Group	Values	NSE	RMSE (%)	MAE (%)	R^2	NSE	RMSE (%)	MAE (%)	R^2
(i)	$a_s = 0.25$, $b_s = 0.50$	0.41	3.43	2.39	0.89	0.51	2.7	1.82	0.89
(ii)	$a_s = 0.25$, $b_s = 0.50$, k	0.74	2.3	0.81	0.78	0.8	1.73	0.26	0.81
(iii)	$a_s = 0.25$, $b_s = 0.65$	0.49	3.18	2.15	0.86	0.6	2.45	1.59	0.87
(iv)	$a_s = 0.25$, $b_s = 0.65$, k	0.75	2.25	0.37	0.75	0.77	1.85	-0.17	0.79
(v)	Monthly coefficients a_s and b_s	0.42	3.41	2.38	0.89	0.52	2.68	1.81	0.89
(vi)	Monthly coefficients a_s and b_s, k	0.74	2.28	0.79	0.78	0.8	1.72	0.24	0.81

*$a_s = 0.25$, $b_s = 0.50$ referred to the result by FAO (Allen et al., 1998); $a_s = 0.25$, $b_s = 0.65$ consulted the research by Liu & Dan (2011); Monthly coefficients a_s and b_s was set as reported by Podesta et al. (2004).

Table 6. The conversion coefficients of various months between D20 evaporation and E601 evaporator.

Month	1	2	3	4	5	6	7	8	9	10	11	12
Conversion coefficients	0.48	0.57	0.46	0.50	0.53	0.54	0.55	0.55	0.59	0.57	0.58	0.58

It was found that the ET_0 existed has linear and positive relationship with ET_{pan}. Meanwhile, due to the lack of the ET_{pan} observation after 2014, ET_0 was used to replace ET_{pan}, and convert it into E601 evaporation pan to evaluate the ET from lake as $ET_{lake} = kp \cdot ET_0$, where kp is the evaporation conversion coefficient of ET_{pan} and E601.

To quantify the daily ET of WL from 2014 to 2016, the monthly coefficients (a_s and b_s) and k were applied to calculating R_n and used PM model to estimate the ET_0 (2014-2016). This method gave annual ET_0 of 1824.34 mm, 1791.98 mm and 1744.84 mm in 2014, 2015, and 2016, respectively. Table 6 showed the conversion coefficients of months between D20 evaporation and E601 evaporator. ET_{lake} were 986.38mm, 956.74mm and 931.35mm in 2014, 2015, and 2016, respectively, with a decreasing trend that was consistent with our finding in Section 3.1.

Estimation of Lake Area and Water Volume Change

Based on the DEM of WL, TM remote sensing data (1995-2017) and lake level observation data (1995-2017), the lake area variations and acquired lake water volume changes were calculated during different phases. Fig. 7 showed the correlation between lake area and corresponding water levels, which shows a strong correlation ($R^2 = 0.82$). With the increment of the water level, the lake area of WL augmented during 1995 to 2017 that was consistent with the results by Chen & Zhao [81]. The increments for WL area and water level were 1.71 km^2 and 0.05 m from 1995 to 2017.

Fig. 8 Water balance derived from observations and model outputs. Precipitation was from Kangping national meteorological station and evaporation was from the retrospective modeling. The negative evaporation presented here indicated water loss from the WL to the atmosphere. Runoff was the monthly runoff and included the surface and groundwater runoff. Water Inflow was the sum of monthly precipitation and runoff into the WL. The change in water was the observations from May to October in 2015 and 2016.

Fig. 8 showed the monthly water balance terms estimated based on the observation data and the retrospective model outputs over 2015 and 2016. The average monthly precipitation was 4.05×10^6 m^3 and 4.97×10^6 m^3 in 2015 and 2016, respectively. The mean monthly runoff was 4.57×10^6 m^3 and 5.18×10^6 m^3 in 2015 and 2016, respectively. The mean monthly total ET_{lake} were 10.35×10^6 m^3 and 10.47×10^6 m^3 in 2015 and 2016, respectively. The average monthly water volume loss was 1.72×10^6 m^3 and 0.33×10^6 m^3 in 2015 and 2016, respectively. The water inflow to the WL

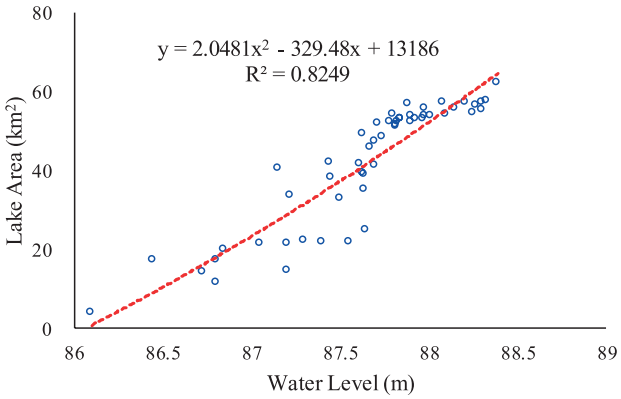

Fig. 7. Scatter plots between water level and lake area.

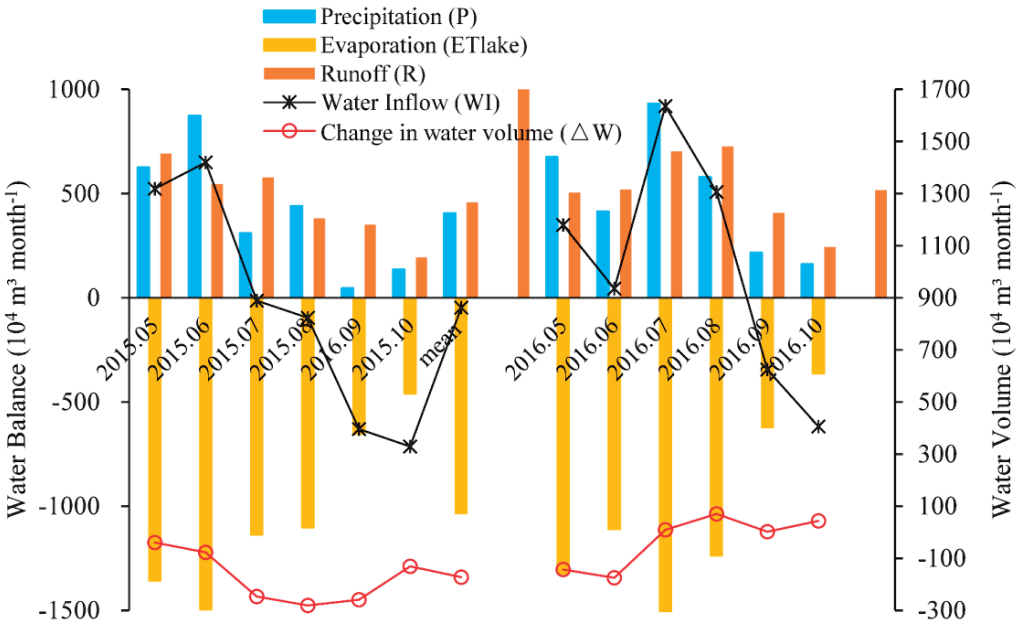

Fig. 8. Water balance derived from observations and model outputs. Precipitation was from Kangping national meteorological station and evaporation was from the retrospective modeling. The negative evaporation presented here indicated water loss from the WL Lake to the atmosphere. Runoff was the monthly runoff and included the surface and groundwater runoff. Water Inflow was the sum of monthly precipitation and runoff into the WL Lake. The change in water was the observations from May to October in 2015 and 2016.

was evaluated from the balance residual by assuming a simplified water balance = $\Delta W + ET_{lake} = P + R$, where ΔW was the change in water volume. The water volume was 8.63×10^6 m³ and 10.14×10^6 m³ in 2015 and 2016. It was found that the lake water inflow could not meet the demand of the evaporation and water volume advancement.

The previous study found that climate changes and human activities had affected on the lake water volume directly or indirectly, which was the critical driving factors for lake evolutions and lake ecological [82, 83]. Zhou et al. announced that temperature augmentation and area construction were the primary driving force in the degradation of lake wetlands [83]. Landes et al. estimated that climatic variation reduced the water surface of wetlands by 5.3%-13.6% during the periods 1961-2000 and 2081-2100 in the Northwest France [84]. As an ecological sensible region for semi-arid zone to humid zone, precipitation and surface runoff were the major input of WL [81]. The water regime was the most imperative ecological element for wetlands. This study suggested that precipitation decrement caused the reduction of water inflow [85]. Otherwise, excessive utilization of water resources caused the loss of water volume. For a closed lake without outflow, given the data-scarce or the lack of observation hydrologic data, water inflow could estimate the water shortage of ecological water demand. Meanwhile, the minimum water demand of lake could be guaranteed with the water inflow available.

Conclusions

In this study, it is found that the annual precipitation, the annual average air temperature, minimum and maximum air temperature, and annual SD shows increasing trends. Contrarily, the annual pan evaporation, WS and RH decreased in WL. Meanwhile, temperature, pan evaporation, and WS changed at the 0.01 significance level. The temperature was the dominant factor for the increment of pan evaporation, followed by WS and SD, while RH showed a decreasing effect on pan evaporation.

ET_0 estimated through PM model shows linear and positive relationship ($R^2 = 0.89$) with ET_{pan}. Then we maintained the coefficient linear regression equation k (k = 1.86) and annual ET_0 of 1824.34 mm, 1791.98 mm and 1744.84 mm in 2014, 2015, and 2016, respectively. And the evaporation on the lake surface was derived as 986.38mm, 956.74mm and 931.35mm in 2014, 2015, and 2016, respectively. The average monthly water volume loss was 1.72×10^6 m³ in 2015 and 0.33×10^6 m³ in 2016. The water inflow to the WL was evaluated by water balance: $\Delta W + ET_{lake} = P + R$. The lake water inflow could not meet the demand of the evaporation and water volume advancement.

This study investigated the ET_0 application in the water inflow of inland plain lake, fill in gaps in the measured hydrological data, especially in the data-scarce and ungauged areas. Meanwhile, this study developed the empirical formula of R_n by utilizing the coefficient, which was derived from data fitting of observational ET_{pan} and estimated ET_0. In sum, our

research is helpful for understanding for planning and management of water resource and irrigation projects.

Due to the limitation of data, only two models were chosen in this study to estimate the ET_0 and calculated less than 3 years water balance in the WL. Using different models may have different results. This study provided an idea for evaluating water balance of the closed-basin lake, especially in the data-scarce or ungauged zones. And if the water inflow did not meet the lake wetlands outflow, extreme climate events, such as drought, could occurr. In this study, the effects of the wetland drought were not considered. In the future, drought evaluation of wetlands utilizing the water balance could be studied prolong.

This study provides a valuable and scientific reference to recognize the water balance in the ungauged inland plain lake. With combined effects of the climatic changes and human activities, wetland protection and restoration measures should be paid more attention. Optimizing the utilities of water resources, such as rainwater harvesting, flood water utilization and seawater desalination [86], could enhance the water inflow of the WL in the future.

Acknowledgments

This research was funded by the [National Natural Science Foundation of China] grant number [52109038 and 51879276]. All researchers are also grateful to the Associate Editor and all reviewers who will propose the constructive comments, which will help greatly to improve our paper.

Conflict of Interest

The authors declare that there is no conflict of interest regarding the publication of this paper.

References

1. VISAKH S., RAJU P.V., KULKARNI S.S., DIWAKAR P.G. Inter-comparison of water balance components of river basins draining into selected delta districts of Eastern India. Sci Total Environ. **654**, 1258, **2019**.
2. LI Z., PAN N., HE Y., ZHANG Q. Evaluating the best evaporation estimate model for free water surface evaporation in hyper-arid regions: a case study in the Ejina basin, northwest China. Environmental Earth Sciences. **75**, (4), **2016**.
3. JOHNSON W.C., POIANI K.A. Climate Change Effects on Prairie Pothole Wetlands: Findings from a Twenty-five Year Numerical Modeling Project. Wetlands. **36** (S2), 273, **2016**.
4. GAO Y., DENG Z., MORRISON A.M. Can Urban Lake Recreational Pressure Be Measured? The Impacts of Urbanization on Wuhan's Lakes. Applied Spatial Analysis and Policy. **12** (2), 255, **2017**.
5. YANG X., WANG N., CHEN A.A., HE J., HUA T., QIE Y. Changes in area and water volume of the Aral Sea in the arid Central Asia over the period of 1960-2018 and their causes. Catena. **191**, 104566, **2020**.
6. BAI M., MO X., LIU S., HU S. Detection and attribution of lake water loss in the semi-arid Mongolian Plateau – A case study in the Lake Dalinor. Ecohydrology. **14** (1), **2020**.
7. XIAO K., GRIFFIS T.J., BAKER J.M., BOLSTAD P.V., ERICKSON M.D., LEE X., WOOD J.D., HU C., NIEBER J.L. Evaporation from a temperate closed-basin lake and its impact on present, past, and future water level. Journal of Hydrology. **561**, 59, **2018**.
8. STAN F.-I., NECULAU G., ZAHARIA L., IOANA-TOROIMAC G., MIHALACHE S. Study on the Evaporation and Evapotranspiration Measured on the Căldăruşani Lake (Romania). Procedia Environmental Sciences. **32**, 281, **2016**.
9. ZHAO X., MEI L., WANG S., LIU Y. Comparison of actual water evaporation and pan evaporation in summer over the Lake Poyang, China. Journal of Lake Sciences. **27** (2), 343, **2015**.
10. HOEGH-GULDBERG O.J.D., TAYLOR M., BINDI M., BROWN S., CAMILLONI I., DIEDHIOU A., DJALANTE R., EBI K.L., ENGELBRECHT F., GUIOT J., HIJIOKA Y., MEHROTRA S., PAYNE A., SENEVIRATNE S.I., THOMAS A., WARREN R., ZHOU G. Impacts of 1.5ºC Global Warming on Natural and Human Systems. In: Global Warming of 15ºC An IPCC Special Report on the impacts of global warming of 15ºC above pre-industrial levels and related global greenhouse gas emission pathways, in the context of strengthening the global response to the threat of climate change, sustainable development, and efforts to eradicate poverty. **2018**.
11. ZHOU J., WANG L., ZHANG Y., GUO Y., HE D. Spatiotemporal variations of actual evapotranspiration over the Lake Selin Co and surrounding small lakes (Tibetan Plateau) during 2003-2012. Science China Earth Sciences. **59** (12), 2441, **2016**.
12. THENG HUE H., NG J.L., HUANG Y.F., TAN Y.X. Evaluation of temporal variability and stationarity of potential evapotranspiration in Peninsular Malaysia. Water Supply. **22** (2), 1360, **2022**.
13. LIU X., YU J., WANG P., ZHANG Y., DU C. Lake Evaporation in a Hyper-Arid Environment, Northwest of China – Measurement and Estimation. Water. **8** (11), 527, **2016**.
14. LIU Y., QIU G., ZHANG H., YANG Y., ZHANG Y., WANG Q., ZHAO W., JIA L., JI X., XIONG Y., YAN C., MA N., HAN S., CUI Y. Shifting from homogeneous to heterogeneous surfaces in estimating terrestrial evapotranspiration: Review and perspectives. Science China Earth Sciences. **65** (2), 197, **2021**.
15. LU X., BAI H., MU X. Explaining the evaporation paradox in Jiangxi Province of China: Spatial distribution and temporal trends in potential evapotranspiration of Jiangxi Province from 1961 to 2013. International Soil and Water Conservation Research. **4** (1), 45, **2016**.
16. GHARBIA S.S., SMULLEN T., GILL L., JOHNSTON P., PILLA F. Spatially distributed potential evapotranspiration modeling and climate projections. Sci Total Environ. **633**, 571, **2018**.
17. CUXART J., BOONE A.A. Evapotranspiration over Land from a Boundary-Layer Meteorology Perspective. Boundary-Layer Meteorology. **177** (2-3), 427, **2020**.

18. OKKAN U., KIYMAZ H. Questioning of empirically derived and locally calibrated potential evapotranspiration equations for a lumped water balance model. Water Supply. **20** (3), 1141, **2020**.
19. XU C.Y. S.V.P. Cross Comparison of Empirical Equations for Calculating Potential Evapotranspiration with Data from Switzerland. Water resources management. **16** (3), 197, **2002**.
20. LEWIS C.S., ALLEN L.N. Potential crop evapotranspiration and surface evaporation estimates via a gridded weather forcing dataset. Journal of Hydrology. **546**, 450, **2017**.
21. LI S., KANG S., ZHANG L., ZHANG J., DU T., TONG L., DING R. Evaluation of six potential evapotranspiration models for estimating crop potential and actual evapotranspiration in arid regions. Journal of Hydrology. **543**, 450, **2016**.
22. LI C., WU P., LI X., ZHOU T., SUN S., WANG Y., LUAN X., YU X. Spatial and temporal evolution of climatic factors and its impacts on potential evapotranspiration in Loess Plateau of Northern Shaanxi, China. Science of the Total Environment. **589**, 165, **2017**.
23. DOUGLAS E.M., JACOBS J.M., SUMNER D.M., RAY R.L. A comparison of models for estimating potential evapotranspiration for Florida land cover types. Journal of Hydrology. **373** (3-4), 366, **2009**.
24. MCCABE G.J., HAY L.E., BOCK A., MARKSTROM S.L., ATKINSON R.D. Inter-annual and spatial variability of Hamon potential evapotranspiration model coefficients. Journal of Hydrology. **521**, 389, **2015**.
25. ALLEN R., PEREIRA L., RAES D., SMITH M., ALLEN R.G., PEREIRA L.S., MARTIN S. Crop Evapotranspiration: Guidelines for Computing Crop Water Requirements, FAO Irrigation and Drainage Paper 56. **1998**.
26. AHOOGHALANDARI M., KHIADANI M., JAHROMI M.E. Calibration of Valiantzas' reference evapotranspiration equations for the Pilbara region, Western Australia. Theoretical and Applied Climatology. **128** (3-4), 845, **2016**.
27. AHMAD M.J., CHOI K.S. Influence of climate variables on FAO Penman–Monteith reference evapotranspiration in the Upper Chenab Canal command area of Pakistan. Paddy and Water Environment. **16** (3), 425, **2018**.
28. THORNTHWAITE C.W. An approach toward a rational classification of climate. Geographical Review. **38** (1), 55, **1948**.
29. HARGREAVES G.H. Moisture Availability and Crop Production. Transactions of the American Society of Agricultural Engineers ASAE. **18** (5), 980, **1975**.
30. RAI R.K., SINGH V.P., UPADHYAY A. Chapter 5 – Estimation of Lake Evaporation and Potential Evapotranspiration. Planning and Evaluation of Irrigation Projects, Academic Press, **2017**.
31. PENMAN H.L. Natural Evaporation from Open Water, Bare Soil and Grass. Proc of the Royal Soc, Series A. **193** (1032), 120, **1948**.
32. ONYUTHA C. Statistical analyses of potential evapotranspiration changes over the period 1930–2012 in the Nile River riparian countries. Agricultural and Forest Meteorology. **226-227**, 80, **2016**.
33. VALIPOUR M., GHOLAMI SEFIDKOUHI M.A., RAEINI−SARJAZ M. Selecting the best model to estimate potential evapotranspiration with respect to climate change and magnitudes of extreme events. Agricultural Water Management. **180**, 50, **2017**.
34. POON P.K., KINOSHITA A.M. Spatial and temporal evapotranspiration trends after wildfire in semi-arid landscapes. Journal of Hydrology. **559**, 71, **2018**.
35. FENG J., YAN D., LI C., YU F., ZHANG C. Assessing the impact of climatic factors on potential evapotranspiration in droughts in North China. Quaternary International. **336**, 6, **2014**.
36. LI B., CHEN F., GUO H. Regional complexity in trends of potential evapotranspiration and its driving factors in the Upper Mekong River Basin. Quaternary International. **380-381**, 83, **2015**.
37. SHWETA YADAV P.D., SONN KUMAR, VANITA PANDEY & PANKAJ KUMAR PANDEY Trends in major and minor meteorological variables and their influence on reference evapotranspiration for mid Himalayan region at east Sikkim. India J Mt Sci. **13**, 302, **2016**.
38. ODONGO V.O., VAN OEL P.R., VAN DER TOL C., SU Z. Impact of land use and land cover transitions and climate on evapotranspiration in the Lake Naivasha Basin, Kenya. Sci Total Environ. **682**, 19, **2019**.
39. ZHENG H., YU G., WANG Q., ZHU X., YAN J., WANG H., SHI P., ZHAO F., LI Y., ZHAO L., ZHANG J., WANG Y. Assessing the ability of potential evapotranspiration models in capturing dynamics of evaporative demand across various biomes and climatic regimes with ChinaFLUX measurements. Journal of Hydrology. **551**, 70, **2017**.
40. FICKLIN D.L., LETSINGER S.L., GHOLIZADEH H., MAXWELL J.T. Incorporation of the Penman-Monteith potential evapotranspiration method into a Palmer Drought Severity Index Tool. Computers & Geosciences. **85**, 136, **2015**.
41. HAN J., WANG J., ZHAO Y., WANG Q., ZHANG B., LI H., ZHAI J. Spatio-temporal variation of potential evapotranspiration and climatic drivers in the Jing-Jin-Ji region, North China. Agricultural and Forest Meteorology. **256-257**, 75, **2018**.
42. KUMMU M., TES S., YIN S., ADAMSON P., JóZSA J., KOPONEN J., RICHEY J., SARKKULA J. Water balance analysis for the Tonle Sap Lake-floodplain system. Hydrological Processes. **28** (4), 1722, **2014**.
43. GIBSON JJ E.P., BIRKS S.J., TWITCHELL C., GRAY C., KARIYEVA J. Isotope-based water balance assessment of open water wetlands across Alberta: Regional trends with emphasis on the oil sands region. Journal of Hydrology: Regional Studies. **40**, 101036, **2022**.
44. LI X.-Y., XU H.-Y., SUN Y.-L., ZHANG D.-S., YANG Z.-P. Lake-Level Change and Water Balance Analysis at Lake Qinghai, West China during Recent Decades. Water resources management. **21** (9), 1505, **2006**.
45. GIBSON J.J., PROWSE T.D., PETERS D.L. Hydroclimatic controls on water balance and water level variability in Great Slave Lake. Hydrological Processes. **20** (19), 4155, **2006**.
46. WALE A., RIENTJES T.H.M., GIESKE A.S.M., GETACHEW H.A. Ungauged catchment contributions to Lake Tana's water balance. Hydrological Processes. **23** (26), 3682, **2009**.
47. XU L. Z.M., HE B., WANG X., ZHANG Q., JIANG J., RAZAFINDRABE B.H.N. Analysis of Water Balance in Poyang Lake Basin and Subsequent Response to Climate Change. Journal of Coastal Research. **68**, **2014**.
48. MA J., WENG B., BI W., YAN D., LI M., XU T., WANG L., WANG L. The Characteristics of Climate Change and Adaptability Assessment of Migratory Bird Habitats in Wolonghu Wetlands. Wetlands. **39** (3), 415, **2018**.

49. YUAN Y., YAN D., WANG H., WANG Q., WENG B. Quantitative assessment of drought in a lacustrine wetland based on a water balance model. Natural hazards. **70** (1), 693, **2013**.
50. FRANZEN L. Can Earth Afford to lose the wetlands in the battle against the increasing greenhouse effect. In: IPC proceedings of the 9th international peat congress. **1992**.
51. KUMANLIOGLU A.A. Characterizing meteorological and hydrological droughts: A case study of the Gediz River Basin, Turkey. **2020**.
52. MARTINUZZI S., ALLSTADT A.J., BATEMAN B.L., HEGLUND P.J., PIDGEON A.M., THOGMARTIN W.E., VAVRUS S.J., RADELOFF V.C. Future frequencies of extreme weather events in the National Wildlife Refuges of the conterminous U.S. **2016**.
53. ZHOU H., KANG S., TONG L., DING R., LI S., DU T. Improved application of the Penman-Monteith model using an enhanced Jarvis model that considers the effects of nitrogen fertilization on canopy resistance. Environmental and Experimental Botany. **159**, 1, **2019**.
54. FORSTER M.A., KIM T.D.H., KUNZ S., ABUSEIF M., CHULLIPARAMBIL V.R., SRICHANDRA J., MICHAEL R.N. Phenology and canopy conductance limit the accuracy of 20 evapotranspiration models in predicting transpiration. Agricultural and Forest Meteorology. **315**, 108824, **2022**.
55. XIANG K., LI Y., HORTON R., FENG H. Similarity and difference of potential evapotranspiration and reference crop evapotranspiration – a review. Agricultural Water Management. **232**, 106043, **2020**.
56. LIU H., LI Y., JOSEF T., ZHANG R., HUANG G. Quantitative estimation of climate change effects on potential evapotranspiration in Beijing during 1951-2010. Journal of Geographical Sciences. **24** (1), 93, **2013**.
57. ZHU L.P., WU X.Y. Quantitative analysis of lake area variations and the influence factors from 1971 to 2004 in the Nam Co basin of the Tibetan Plateau. Science Bulletin. **55** (13), 1294, **2010**.
58. ISMAIL S.M., EL-NAKHLAWY F.S. Measuring Crop Water Requirement and Crop Coefficient for Blue Panic Crop Under Arid Conditions Using Draining Lysimeters. Irrigation and Drainage. **67** (3), 454, **2018**.
59. BORNEMANN N., NIEMANN S., STETTNER S., MORGENSTERN A., LANGER M., BOIKE J. Quantification of a full year water balance of a thermokarst lake in East Siberia based on field measurements. Humboldt-Universität zu Berlin: Quantification of a full year water balance of a thermokarst lake in East Siberia based on field measurements , XI. International Conference on Permafrost, Potsdam, **2016**.
60. LIU W., WANG L., ZHOU J., LI Y., SUN F., FU G., LI X., SANG Y.-F. A worldwide evaluation of basin-scale evapotranspiration estimates against the water balance method. Journal of Hydrology. **538**, 82, **2016**.
61. NOVÁK V. Evapotranspiration in the Soil-Plant-Atmosphere System. Springer Netherlands, Press in Soil Science, **2012**.
62. NASH J.E., SUTCLIFFE J.V. River flow forecasting through conceptual models part I — A discussion of principles. J Hydrol. **10** (3), 282, **1970**.
63. ALADENOLA O.O., MADRAMOOTOO C.A. Evaluation of solar radiation estimation methods for reference evapotranspiration estimation in Canada. Theoretical and Applied Climatology. **118** (3), 377, **2013**.
64. MOTOVILOV Y.G., GOTTSCHALK, L., ENGELAND, K., RODHE, A. Validation of a distributed hydrological model against spatial observations. Agricultural and Forest Meteorology. **98-99**, **1999**.
65. LEI X., YIN J., YUAN Z., WANG R., CAI S., YU Y., LI H. The Long-term Projection of Surface Runoff in the Regions above Danjiangkou in Hanjiang River Basin based on Water-energy Balance. MATEC Web of Conferences. **246**, 01099, **2018**.
66. YANG H., YANG D. Climatic factors influencing changing pan evaporation across China from 1961 to 2001. Journal of Hydrology. **414-415**, 184, **2012**.
67. HE G., ZHAO Y., WANG J., GAO X., HE F., LI H., ZHAI J., WANG Q., ZHU Y. Attribution analysis based on Budyko hypothesis for land evapotranspiration change in the Loess Plateau, China. Journal of Arid Land. **11** (6), 939, **2019**.
68. YANG F., ZHANG Q., WANG R., ZHOU J. Evapotranspiration measurement and crop coefficient estimation over a spring wheat Farmland ecosystem in the Loess Plateau. Plos One. **9** (6), e100031, **2014**.
69. FENG Y., JIA Y., ZHANG Q., GONG D., CUI N. National-scale assessment of pan evaporation models across different climatic zones of China. Journal of Hydrology. **564**, 314, **2018**.
70. FAN, ZX, THOMAS Spatiotemporal variability of reference evapotranspiration and its contributing climatic factors in Yunnan Province, SW China, 1961-2004. Climatic Change. **116** (2), 309, **2013**.
71. SOROUSH F., FATHIAN F., KHABISI F.S.H., KAHYA E. Trends in pan evaporation and climate variables in Iran. Theoretical and Applied Climatology. **142** (1-2), 407, **2020**.
72. MARTí P., ZARZO M., VANDERLINDEN K., GIRONA J. Parametric expressions for the adjusted Hargreaves coefficient in Eastern Spain. Journal of Hydrology. **529**, 1713, **2015**.
73. TEGOS A., EFSTRATIADIS A., MALAMOS N., MAMASSIS N., KOUTSOYIANNIS D. Evaluation of a Parametric Approach for Estimating Potential Evapotranspiration Across Different Climates. Agriculture and Agricultural Science Procedia. **4**, 2, **2015**.
74. MAKIN M. K.T., WADDAMS A., BIRCHALL C., EAVIS B. Prospects for irrigation development around Lake Zwai, Ethiopia. Land Resources Division, Surbiton, Surrey (England), **1976**.
75. LOUCHE A., NOTTON G., POGGI P., SIMONNOT G. Correlations for direct normal and global horizontal irradiation on a French Mediterranean site. Solar Energy. **46** (4), 261, **1991**.
76. SUPIT I., E. V.D.G. Updated system description of the WOFOST crop growth simulation model as implemented in the crop growth monitoring system applied by the European Commission. Internet On-line Book. Trebook 7. Heelsum, The Netherlands: Treemail Publishers, **2003**.
77. PODESTÁ G.P., NÚÑEZ L., VILLANUEVA C.A., SKANSI M.A.A. Estimating daily solar radiation in the Argentine Pampas. Agricultural and Forest Meteorology. **123** (1-2), 41, **2004**.
78. FU G., LIU C., CHEN S., HONG J. Investigating the conversion coefficients for free water surface evaporation of different evaporation pans. Hydrological Processes. **18** (12), 2247, **2004**.
79. ABTEW W., MELESSE A. Evaporation and Evapotranspiration. Springer, **2012**.
80. CHEN H., ZHAO Y.W. Evaluating the environmental flows of China's Wolonghu wetland and land use changes using a hydrological model, a water balance model, and remote sensing. Ecological Modelling. **222** (2), 253, **2011**.

81. ZHAO D., HE H., WANG W., WANG L., DU H., LIU K., ZONG S. Predicting Wetland Distribution Changes under Climate Change and Human Activities in a Mid- and High-Latitude Region. Sustainability. **10** (3), 863, **2018**.
82. ZHOU B., YIN J., JIN B., ZHU L. Degradation of Wuchang Lake wetland and its causes during 1980-2010. Acta Geographica Sinica. **69** (11), 1697, **2014**.
83. LANDES A.A.L., AQUILINA, L., RIDDER, J. D., LONGUEVERGNE, L., PAGé, C., GODERNIAUX, P. Investigating the respective impacts of groundwater exploitation and climate change on wetland extension over 150 years. Journal of Hydrology. **509** (2), 367, **2014**.
84. SHADKAM S., LUDWIG F., OEL P.V., KIRMIT Ç., KABAT P. Impacts of climate change and water resources development on the declining inflow into Iran's Urmia Lake. Journal of Great Lakes Research. **42** (5), **2016**.
85. YUAN Z., YAN D., YANG Z., XU J., HUO J., ZHOU Y., ZHANG C. Attribution assessment and projection of natural runoff change in the Yellow River Basin of China. Mitigation and Adaptation Strategies for Global Change. **23** (1), 227, **2018**.